

Evidence for clustered mannose as a new ligand for hyaluronan-binding protein (HABP1) from human fibroblasts

RAJEEV KUMAR, NIRUPAM ROY CHOUDHURY[†], DINAKAR M SALUNKE[§] and K DATTA*

Biochemistry Laboratory, School of Environmental Sciences, [†]Genetic Engineering Unit, Jawaharlal Nehru University, New Delhi 110 067, India

[§]National Institute of Immunology, Aruna Asaf Ali Marg, New Delhi 110 067, India

**Corresponding author (Fax, 91-11-6165886; Email, datta_k@hotmail.com).*

We have earlier reported that overexpression of the gene encoding human hyaluronan-binding protein (HABP1) is functionally active, as it binds specifically with hyaluronan (HA). In this communication, we confirm the collapse of the filamentous and branched structure of HA by interaction with increasing concentrations of recombinant-HABP1 (rHABP1). HA is the reported ligand of rHABP1. Here, we show the affinity of rHABP1 towards D-mannosylated albumin (DMA) by overlay assay and purification using a DMA affinity column. Our data suggests that DMA is another ligand for HABP1. Furthermore, we have observed that DMA inhibits the binding of HA in a concentration-dependent manner, suggesting its multiligand affinity amongst carbohydrates. rHABP1 shows differential affinity towards HA and DMA which depends on pH and ionic strength. These data suggest that affinity of rHABP1 towards different ligands is regulated by the microenvironment.

1. Introduction

We have earlier reported the identification of a novel glycoprotein from different rat tissues, which has a specific affinity towards hyaluronan (HA) (Gupta *et al* 1991). It was further demonstrated that hyaluronan-binding protein (HABP1) binds specifically to HA amongst glycosaminoglycans (GAGs) with a K_d 10^{-9} M in a positively cooperative manner (Gupta *et al* 1991). The clone encoding HA-binding protein has been isolated by immunoscreening the human fibroblast expression library with anti-HABP1 amino acid and confirmed by comparing the predicted internal antibody sequence with that of the purified protein (Deb and Datta 1996). Sequence analysis of the gene encoding HABP1 confirmed this protein to be a member of Hyaladherin family, as it contains the HA-binding domain. The overexpressed biotinylated recombi-

nant-HABP1 (rHABP1) binds to HA and could be competed with unlabelled HABP1, suggesting that it is the functionally active form. Crystal structure of p32/HABP1 (Jiang *et al* 1999) also confirmed the presence of an exposed HA-binding site. The HABP1 gene is localized on human chromosome 17p12-p13 (Majumder and Datta 1998). This protein appears to be a multifunctional protein having identical sequence homology with the receptor for globular head of C1q and p32, a protein co-purified with human splicing factor 2 (SF2) and YL-2 (Das *et al* 1997).

Recently, the solution structure of another member of Hyaladherin family, TSG-6 was also found to be a calcium dependent (C-type) lectin (Kohda *et al* 1996), which was first detected in rat and named mannose-binding protein (MBP) (Parker *et al* 1998). The putative HA-binding site of TSG6 is topologically similar to that in HABP1

Keywords. Hyaluronan; hyaluronan binding protein; D-mannosylated albumin

Abbreviations used: BCIP, 5-bromo-4-chloro-3-indolyl phosphate; f-BSA, formaldehyde treated bovine serum albumin; CRD, Carbohydrate recognition domain; DAB, 3'3'-Diamino-benzidine; DMA, D-mannosylated albumin; EDC, 1-ethyl-3-(diethylamino-propyl) carbodiimide hydrochloride; GAGs, glycosaminoglycans; HA, hyaluronan; HABP1, hyaluronan binding protein; HRP, horse radish peroxidase; MBP, mannose binding protein; NBT, nitroblue tetrazolium; OPD, O-phenylene diamine; PBST, PBS with 0.05% Tween 20; PTR, proteoglycan tandem repeat.

(Kohda *et al* 1996) and CD44 (Bajorath *et al* 1998). This site is seen to correspond to the carbohydrate-binding site in E-selectin, which has similarity in the three-dimensional structure of MBP. This raises the possibility of HABP1 having mannose as another ligand. Thus, in the present communication, we examined if rHABP1 has any affinity towards D-mannosylated albumin (DMA).

2. Materials and methods

2.1 Rotary shadowing electron microscopy

Hyaluronic acid was dissolved in PBS and dialyzed overnight against PBS at 4°C to remove contaminating short hyaluronate oligosaccharides. Hyaluronic acid (500 µg/ml) alone or with rHABP1, at different concentration (0.1 µg, 1.0 µg, 10 µg, 100 µg and 500 µg/ml) were incubated overnight at 4°C. Ten µl of the preincubated sample was adsorbed on carbon coated copper grid (400 mesh) for 5 min at room temperature. The grids were subsequently washed with distilled water and were then mounted on a motor-driven horizontal table rotating at 120 rpm in a vacuum chamber. After evacuation of the chamber to 2×10^{-5} torr, the sample was shadowed with platinum (8 cm of 0.02 mm, 7 to 7.4 V) at an angle of 6° to 9° for 15 s. Finally, grids were examined in a Philips EM 410 transmission electron microscope, operating at 60 kV with 200 µm condenser aperture and 40 µm objective aperture. Pictures were taken on Kodak 4463 EM film.

2.2 Purification of rHABP1 and raising anti-rHABP1-polyclonal antibody

rHABP1 was purified and polyclonal antibodies were raised according to the method described earlier (Deb and Datta 1996). In short, extract of BL21 (DE3) *Escherichia coli* cells overexpressing rHABP1 was centrifuged and the supernatant was dialyzed against 20 mM Tris-HCl, pH 8.5. The extract was loaded onto the ResourceTM-Q column (Pharmacia, Uppsala, Sweden) at a rate of 0.5 ml/min. After washing the column, the bound protein was eluted with the same buffer containing high salt (0.6 M NaCl) and the eluate was dialyzed overnight against PBS at 4°C and stored.

2.3 Preparation of DMA and formaldehyde treated albumin

The DMA was prepared by coupling *p*-aminophenyl-**a**-D-mannopyranoside to bovine serum albumin (BSA) through water soluble 1-ethyl-3-(diethylaminopropyl)-carbodiimide hydrochloride (EDC) as described earlier (Lonngren and Goldstein 1978). Briefly, BSA (27.13 mg) was added

to a 6 ml stirring solution of *p*-aminophenyl **a**-D-mannopyranoside (136 mg) in water (pH 4.75). To this solution 1 ml solution of EDC (155 mg) was added drop wise over a period of 30 min at room temperature (pH 4.75) and allowed to stand for 6 h. The reaction was stopped by the addition of 1 M sodium acetate buffer (pH 5.5) and the solution was dialyzed exhaustively against water prior to recovery by freeze drying. Final freeze dried product was assayed for mannose bound per mol of albumin and it was found to be 20 mol of mannose per mol of albumin. Formaldehyde treated BSA was prepared by using the method described by Mego and McQueen (1995). BSA (500 mg) was dissolved in 50 ml 0.2 M Na₂CO₃, pH 10.0, formaldehyde was added to a final concentration of 20% and was stirred for 72 h in the dark at room temperature. The solution was filtered over a 0.2 µm filter to remove insoluble material, purified on a Sephadex G-25 column, washed with distilled water on a PM-10 membrane in an Amicon[®] stirred cell concentrator and finally lyophilized.

2.4 Preparation of DMA-sepharose affinity column

CH Sepharose (Pharmacia) was coupled to BSA-mannose using water-soluble carbodiimide (EDC) according to the manufacturer's protocol. Briefly, CH Sepharose (1.5 ml) was coupled with unblocked BSA-mannose (58 mg) in the presence of EDC (80 mg) in total volume of 3.0 ml water overnight at pH 4.5–6.0. Unblocked BSA-mannose was prepared without acetate buffer treatment in BSA-mannose preparation. After coupling, acetate buffer treatment was done. BSA-mannose Sepharose column was then equilibrated with PBS at 4°C and *E. coli* lysate containing rHABP1 was loaded and washed with ten bed volumes each of PBS followed by high salt wash. The protein bound to BSA-mannose column was then eluted with 0.2 M Glycine-HCl (pH 2.2) and the eluate was dialyzed overnight against PBS at 4°C followed by analysis on 12.5% non reducing SDS-PAGE and Western transfer followed by immunodetection using polyclonal anti-rHABP1 antibodies.

2.5 Preparation of rHABP1-HRP conjugate

rHABP1 was conjugated to horse radish peroxidase (HRP) by using glutaraldehyde as crosslinker. After dialysis, the rHABP1-HRP conjugate was separated from the free HRP by gel permeation chromatography on a pre-calibrated Superose 6 column with PBS. The purified rHABP1-HRP conjugate was stored at –20°C in 1% BSA and 50% glycerol.

2.6 Immunoblot-binding assays

Equal amounts of DMA and f-BSA were separated on 12.5% SDS-PAGE and transblotted onto a nitrocellulose membrane (Towbin *et al* 1979). The membrane contain-

ing DMA and the control were blocked in PBS with 0.05% Tween20 (PBST) containing 3% BSA for 2 h at 37°C followed by washes. Membrane was incubated in PBS containing 100 µg/ml of rHABP1 for 2 h at 37°C followed by several washes with PBST. Bound rHABP1 was immunodetected using rabbit anti-rHABP1 antibodies (1 : 1000) and visualized by nitroblue tetrazolium (NBT)/5-bromo-4-chloro-3-indolyl phosphate (BCIP) detection system (Promega, Madison, USA) using goat anti-rabbit alkaline phosphatase conjugate as secondary antibody (1 : 7500).

2.7 Solid phase-binding assay

Binding of the rHABP1-HRP conjugate to DMA or HA and inhibition by GAGs and DMA were determined on polystyrene wells of microtitre plates (Costar, Corning, NY, USA). For that purpose, DMA (0.025 µg–15 µg/well) in 0.1 M Na₂CO₃ (pH 9.6) was adsorbed on the wells of microtitre plates and incubated at 4°C for 16 h. After aspirating the residual DMA solution, plates were washed with PBST and blocked with BSA. For coating HA, the microtitre plates were pre-treated with 0.01% (w/v) protamine sulphate at room temperature for 90 min and washed with distilled water. Then, HA (20 µg/100 µl/well) was adsorbed and incubated at 4°C for 16 h. Plates were washed with PBST and blocked with 2% BSA. They were subsequently incubated with rHABP1-HRP conjugate (for binding assays) or with a pre-incubated mixture of conjugate and inhibitors (for binding inhibition assays), after several washes with PBST. The pre-incubation of the rHABP1-HRP conjugate for binding inhibition assays was carried out by mixing equal volumes of the conjugate and the inhibitor at varying concentrations. After 1 h at 37°C, the conjugate inhibitor mixture (100 µl) was added to wells coated with HA (20 µg/well), in triplicate and the plates were incubated for 2 h at 37°C. The plates were washed with PBST, and the bound rHABP1-HRP was estimated using O-phenylene diamine (OPD)-peroxidase reaction. The colour developed in the ELISA was determined at 490 nm in the linear portion of the colorimetric assay.

2.8 Colorimetric assay for carbohydrate derivatized beads

A portion of resin that contained equal amount of beads coupled to BSA-mannose, mannose, BSA and uncoupled CH sepharose were taken separately and washed thrice with PBST for 10 min. The beads were then incubated for 30 min at 37°C in PBST containing 3% BSA and washed thrice with PBST for 5 min. The beads were incubated with rHABP1-HRP conjugate (32 ng/ml) in PBST containing 1% BSA at 37°C for 2 h and then washed thrice

with PBST for 5 min (Liang *et al* 1997). Resin was stained using 3'3'-Diamino-benzidine (DAB) (6 mg DAB in 10 ml of PBS supplemented with 6 µl H₂O₂) and photographed using Nikon Labophot Microscope.

3. Results

3.1 Change in network structure of HA by interaction with HABP1

For functional characterization of rHABP1, filament structure of HA was examined by allowing it to react with varying concentrations of HABP1. As shown by electron micrograph in the absence of rHABP1, HA (500 µg/ml) filaments accentuated the extensive nature of networks and highlighted the multiple branch points (figure 1A). When same concentration of HA (500 µg/ml) was incubated with increasing concentrations of rHABP1 (0.1–500 µg/ml), it leads to a decrease in branching point and network of HA in a concentration dependent manner up to 10 µg/ml (figure 1B, C, D). Further increase in concentration of rHABP1 (100 µg, 500 µg/ml), with the same concentration of HA (500 µg/ml), leads to a collapse of the filamentous and branched structure into large aggregates (figure 1E, F).

3.2 Mannosylated BSA as a novel ligand for rHABP1

Varying concentrations of DMA and f-BSA were electrophoresed and then transferred onto a nitrocellulose membrane and probed with rHABP1. The bound rHABP1 was immunodetected with antibodies against rHABP1. As shown in figure 2, rHABP1 binds only to DMA in a concentration dependent manner (lanes 4–6) but not to f-BSA (lanes 1–3). Primary antibody (rabbit anti-rHABP1) and secondary antibody (goat anti-rabbit alkaline phosphatase conjugate) were used in the negative control blot, in the same dilution, without probing it with rHABP1. It shows no binding to either DMA or f-BSA (data not shown) confirming that DMA binds to rHABP1 in a ligand specific manner but not to the primary and secondary antibodies.

In order to further examine the affinity of rHABP1 towards DMA, an attempt was made to purify *E. coli* over-expressed rHABP1 using DMA as the affinity matrix. This was compared with the purification of rHABP1 using HA-Sepharose affinity column. The protein purified by both the procedures was detected with antibody against rHABP1. As evident from figure 3, both the procedures, as expected, resulted in comparable yields of pure rHABP1 of 34 kDa, using HA-Sepharose (lane 1) and DMA as affinity matrix (lane 2).

Our observation on the specific binding of rHABP1 to DMA led us to examine whether its affinity is dependent

on the spatial distribution of mannose residues. As shown in (figure 4A), rHABP1-HRP shows interaction, only with DMA derivatized beads by precipitating an insoluble brown polymer as a result of peroxidase DAB staining. However, mannose derivatized (figure 4B), BSA (figure 4C) and non-derivatized beads (figure 4D) did not get

stained. Beads that stain darkly, presumably have more enzyme-linked conjugate, which is directly linked to bound rHABP1. As a positive control, HA derivatized beads also show binding with rHABP1-HRP conjugate (like DMA derivatized beads). This data suggests the specificity of rHABP1-HRP conjugate for DMA showing

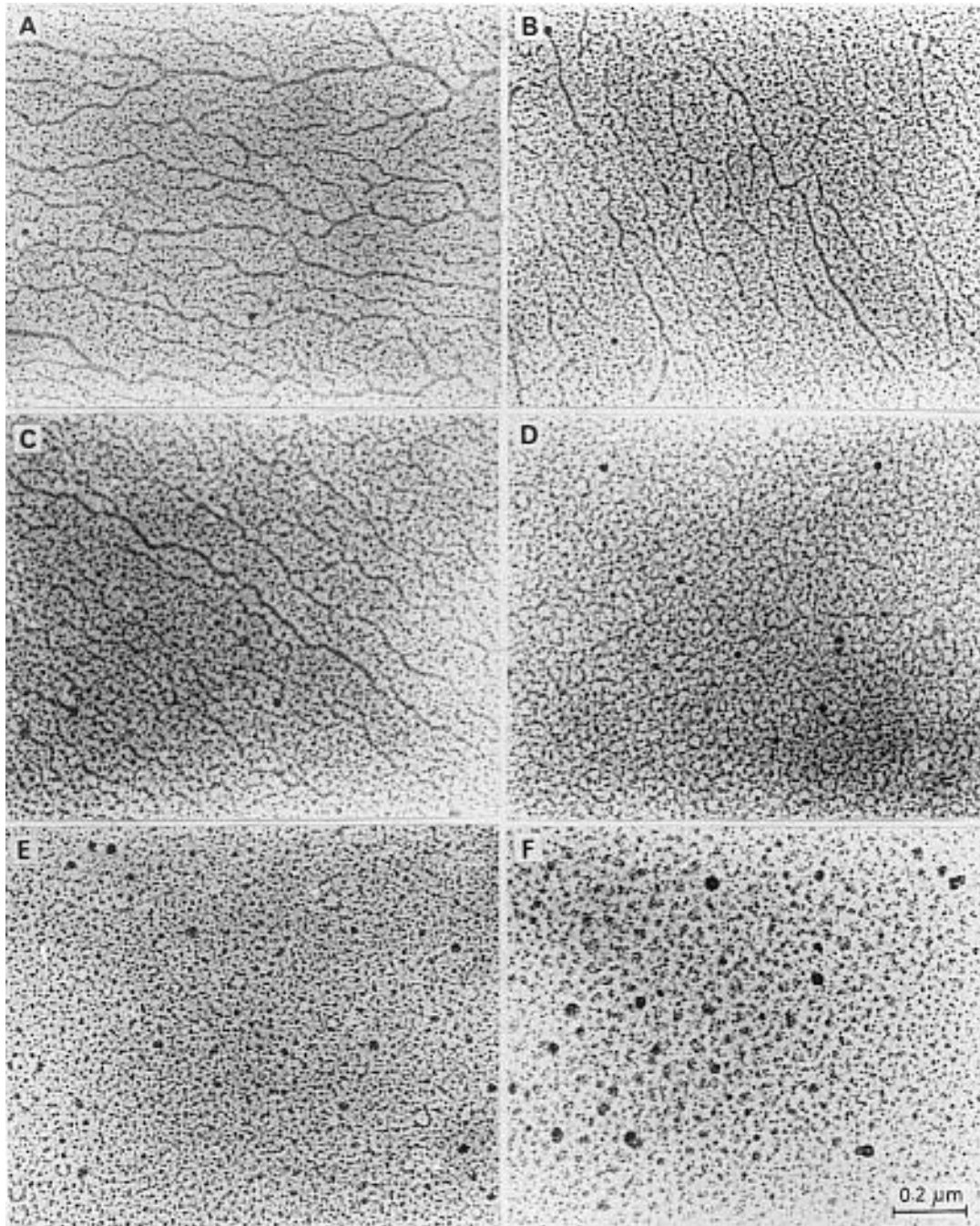


Figure 1. Collapse of HA network as a result of HA-rHABP1 interaction. Electron micrography after rotary shadowing of HA alone (500 µg/ml) (A) or incubated with varying concentrations of rHABP1, 0.1 µg/ml (B), 1 µg/ml (C), 10 µg/ml (D), 100 µg/ml (E) and 500 µg/ml (F).

that rHABP1 binds only to clustered mannose presented on the backbone of protein but not to either mannose monomer or protein backbone.

3.3 Comparative analysis of the interaction of rHABP1 with HA and DMA

In order to quantitatively analyse the interaction of rHABP1 with different ligands, rHABP1 was conjugated to a stable enzyme HRP and the rHABP1-HRP conjugate was purified. This conjugate has the advantage over the immunodetection system as it can be used directly in ELISA as soluble chromophore. Therefore, the rHABP1-HRP conjugate was used for comparing the HABP1 binding with hyaluronic acid and DMA. As represented in figure 5A, DMA immobilized on ELISA plate can bind with rHABP1 (16 ng/ml) in a concentration dependent manner and a higher amount of bound rHABP1-HRP is detected if the concentration of rHABP1 is doubled. The sigmoidal shape of the curve, illustrating the binding of rHABP1 with DMA suggests the co-operative nature of their interaction. In addition, the specific affinity of rHABP1 towards DMA is fully confirmed since there is no binding when rHABP1-HRP is pre-incubated with 20 fold excess of unlabelled rHABP1. An identical sigmoidal profile of binding of rHABP1 to DMA was also obtained when bound rHABP1 was detected by rabbit anti-rHABP1 antibodies followed by goat anti-rabbit HRP conjugate suggesting that conjugation of HRP to rHABP1 does not alter the biochemical nature of rHABP1 (data not shown).

To compare the affinity of rHABP1 to different ligands, HA (20 µg/ml) was immobilized and incubated with rHABP1-HRP conjugate pre-incubated with varying concentrations of either DMA or HA or other GAGs. Subsequently, the rHABP1-HRP bound to immobilized HA

was measured colorimetrically. As evident from figure 5B, the binding of rHABP1 to immobilized HA could be inhibited only by soluble HA and DMA, but not with any other soluble GAGs e.g. glucuronic acid, chondroitin-4-sulphate, N-acetyl-glucosamine or heparin. The profile depicting inhibition of rHABP1 binding to immobilized HA is more by pre-treatment with DMA in comparison to HA, suggesting that rHABP1 has higher affinity towards DMA compared to HA.

In order to examine if the affinity of HABP1 to its ligands is regulated by the micro-environmental factors such as pH and ionic strength, we studied the interaction of HABP1 with either HA or DMA at different ionic strengths (figure 5C) and pH (figure 5D) conditions. The binding of rHABP1 to HA is dependent on ionic strength as optimal binding of this protein to HA is seen only in the presence of NaCl (150–500 mM). However, the presence of same concentration of NaCl inhibits the binding of HABP1 with DMA. The maximum binding of rHABP1 with DMA was seen at 100 mM concentration of NaCl. The affinity of rHABP1 towards DMA was maximum at pH 6.0, whereas the same for HA was at pH 7.2 (figure 5D). This data suggests that these two factors determine the differential binding of rHABP1 with HA or DMA.

4. Discussion

In this communication, we confirm the functionality of rHABP1 as HA receptor by observing the collapse in the filamentous structures of HA by interacting with HABP1 under electron microscope. In addition to HA, we have further shown that HABP1 has DMA as another ligand. This was concluded on the basis of the following observations. Firstly, the specific affinity of HABP1 to DMA is concentration dependent and sensitive to the spatial distribution of the mannose clusters. Secondly, cooperative interaction of HABP1 with varying concentration of DMA is seen. Thirdly, pre-incubation of rHABP1 with DMA inhibits its binding with HA and finally, HABP1 interaction with these two ligands is dependent on pH and ionic strength of the buffer.

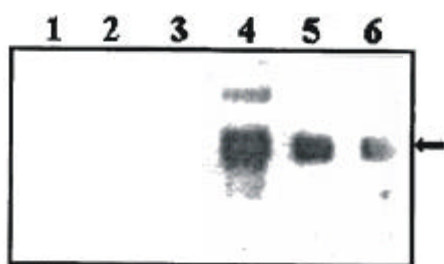


Figure 2. Specific affinity of rHABP1 towards DMA. Formaldehyde treated BSA (f-BSA) (lane 1, 5 µg; lane 2, 2 µg; lane 3, 1 µg) and DMA (lane 4, 5 µg; lane 5, 2 µg; lane 6, 1 µg) were separated on SDS-PAGE and transblotted onto nitrocellulose and probed with the rHABP1. Bound rHABP1 was immunodetected with anti-rHABP1 antibodies and visualized following the protocol described in the NBT/BCIP detection kit. The arrow indicates the band which interact to rHABP1

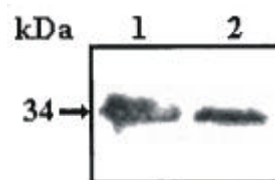


Figure 3. Evidence for the affinity of DMA towards rHABP1. Immunodetection of rHABP1, purified by HA-affinity chromatography (lane 1) and DMA-affinity chromatography (lane 2), by antibodies specific for rHABP1.

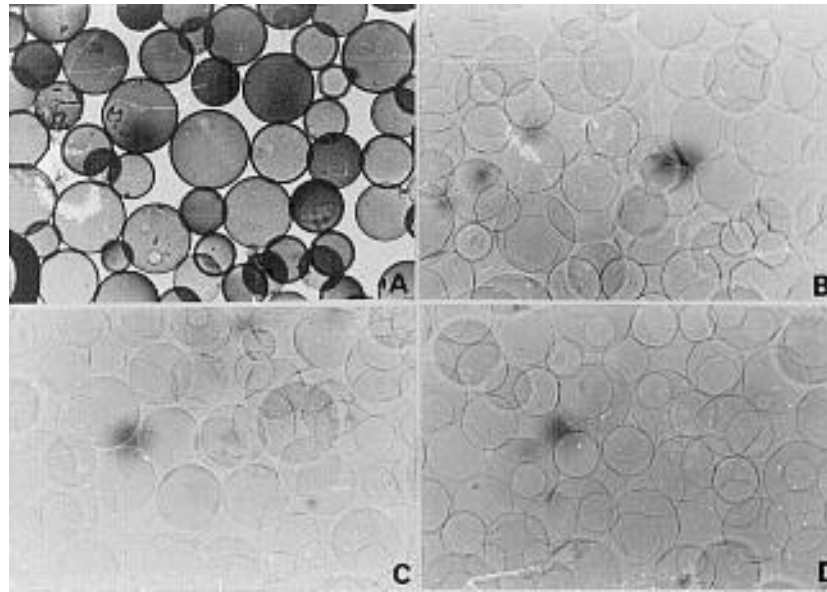


Figure 4. Colorimetric assay showing spatial distribution sensitive binding of rHABP1 to mannose residues. rHABP1-HRP conjugate was incubated with CH sepharose bead derivatized with DMA (A), mannose (B), BSA (C) or underivatized (D) and the bound rHABP1-HRP was detected by staining the beads with DAB.

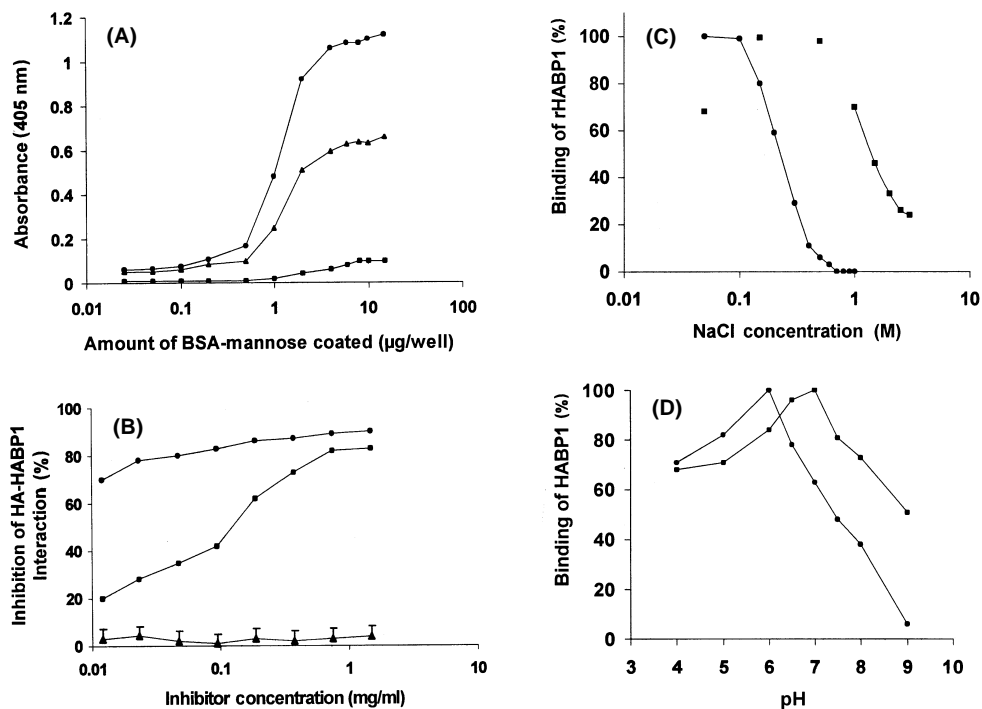


Figure 5. rHABP1 interaction with DMA. (A) Varying concentration of DMA is coated on microtitre plate and incubated with rHABP1-HRP conjugate at concentration of 16 ng/ml (-▲-), 32 ng/ml (-●-), and 32 ng/ml preincubated 20-fold unlabelled rHABP1 (-■-). The bound rHABP1 was detected as described. (B) Comparative analysis on the affinity of rHABP1 towards HA, DMA and other GAGs. rHABP1-HRP conjugate (32 ng/ml) was preincubated with different concentrations of DMA (-●-), HA (-■-) and GAGs (-▲-) loaded on microtitre wells coated with fix HA (20 µg/100 µg/well) and the bound rHABP-HRP conjugate was detected by OPD-peroxidase reaction. The values represent the average of the individual data for each of the four GAGs (chondroitin sulphate, glucuronic acid, N-acetyl glucosamine, and heparin). (C) Effect of ionic strength and (D) pH on the binding of rHABP1-HRP conjugate to HA and DMA depends on ionic strength. rHABP1-HRP conjugate (32 ng/ml) was bound to microtitre wells coated with fixed amount of HA (-■-) (20 µg/100 µl/well) and DMA (-●-) (5 µg/100 µl/well) at different NaCl concentration or pH as indicated, and binding was detected by OPD-peroxidase reaction.

The fact that rHABP1 binds specifically to DMA, but not to BSA or mannose, suggests that its binding to mannose is sensitive to the spatial density and arrangement of the mannose moieties. This is a specific feature of mannose-binding proteins, which prefer mannose in a clustered form (20–23 residues) on a protein backbone rather than in the monosaccharide form (Youssef *et al* 1996; White *et al* 1995). Several observations have shown the significance of multivalent DMA as a more effective ligand than D-mannose. The final spatial arrangement or preferred cluster conformation of multiple residues could well prove to be critical for the high affinity binding of natural oligosaccharides, confirming similar findings with other animal lectins and their corresponding ligands (Lee and Lee 1987, Lee *et al* 1992).

The specific binding of rHABP1 to HA among GAGs is consistent with our earlier observation with tissue HABP1 (Gupta *et al* 1991). Binding of rHABP1 to HA can be blocked effectively by DMA in a concentration dependent manner, suggesting the dual affinity of rHABP1 for HA and DMA. Dual affinity shown by HABP1 for HA and clustered mannose is not unexpected, since the protein fold of HA-binding proteoglycan tandem repeat (PTR) domain is similar to the carbohydrate recognition domain (CRD) of mannose-binding C-type lectin (Brissett and Perkins 1996). However, the differential affinity of HABP1 to HA and DMA as well as the requirement of different ionic strengths for those two ligands may provide an intricate regulatory role in determining the ligand to be chosen.

Our present observation on the identification of mannose-ylated albumin as the novel ligand of HABP1, a cell surface protein, needs a special attention. C-type animal lectins and mannose-binding proteins mediate several different types of interactions at the cell surface. If both the lectins and their carbohydrate ligands are components of mammalian cell surfaces, sugar recognition can form the basis for cell adhesion (Drickmer 1988). The characteristic of HABP1 as cell adhesive protein on macrophage cell surface is already documented (Gupta and Datta 1991). In addition to recognizing endogenous sugar structures, certain C-type lectins have high affinity for saccharides, which form part of the surface of bacterial and fungal pathogens. So mannose rich structures on these organisms may play an important role in innate immunity (Stahl 1990).

Another critical role of clustered mannose residues, is to mediate sperm oocyte interaction through zona pellucida (Tulsiani 1997). Mannose residues of ZP3 in a spatial arrangement is proposed to bind on the sperm surface and a significant correlation between the expression of mannose ligand receptors on sperm and fertilization potential *in vitro* is reported (Benoff *et al* 1993). It is important to mention that we have already reported the

localization of HABP1 on sperm surface and the inhibition of sperm oocyte interaction by anti HABP1 antibody (Ranganathan *et al* 1994). Thus, our present observation on mannose cluster as a novel ligand for HABP1 opens a new avenue for functional aspects of HABP1.

References

- Bajorath J, Greenfield B, Muro S B, Day A J and Aruffo A 1998 Identification of CD44 residues important for hyaluronan binding and delineation of the binding site; *J. Biol. Chem.* **273** 338–343
- Benoff S, Cooper G W, Hurley I, Rosenfeld D L, Schooll G H and Napolitano B 1993 Human fertilizing potential *in vitro* is correlated with differential expression of a head specific mannose ligand receptor; *Fertil. Steril.* **59** 854–862
- Brissett N C and Perkins S J 1996 The protein fold of the hyaluronate-binding proteoglycan tandem repeat domain of link protein, aggrecan and CD44 is similar to that of the C-type superfamily; *Fed. Eur. Biochem. Soc. Lett.* **388** 211–216
- Das S, Deb T B, Kumar R and Datta K 1997 Multifunctional activities of human fibroblast 34-kDa hyaluronic acid-binding protein; *Gene* **190** 223–225
- Deb T B and Datta K 1996 Molecular cloning of human fibroblast hyaluronic acid binding protein confirms its identity with P-32, a protein copurified with splicing factor SF2; *J. Biol. Chem.* **269** 2206–2212
- Drickmer K 1988 Two distinct classes of carbohydrate recognition domains in animal lectin; *J. Biol. Chem.* **263** 9557–9562
- Gupta S, Babu B R and Datta K 1991 Purification, partial characterization of rat kidney hyaluronic acid binding protein and its localization on the cell surface; *Eur. J. Cell Biol.* **56** 58–67
- Gupta S and Datta K 1991 Possible role of hyaluronectin on cell adhesion in rat histiocytoma; *Exp. Cell Res.* **195** 386–394
- Jiang J, Zhang Y, Krainer A R and Xu R 1999 Crystal structure of human p32, a doughnut-shaped acidic mitochondrial matrix protein; *Proc. Natl. Acad. Sci. USA* **96** 3572–3577
- Kohda D, Morton C J, Parkar Hatanaka H, Inagaki F M, Campbell I D and Day A J 1996 Solution structure of the linker module: a hyaluronan-binding domain involved in extracellular matrix stability and cell migration; *Cell* **86** 767–775
- Lee R T and Lee Y C 1987 Affinity labeling of the galactose N-acetylgalactosamine specific receptor of rat hepatocytes: preferential labeling of one of the subunits; *Biochemistry* **26** 6320–6329
- Lee R T, Ichikawa Y, Kawasaki T, Drickmer K and Lee Y C 1992 Multivalent ligand binding by serum mannose-binding protein; *Arch. Biochem. Biophys.* **299** 129–136
- Liang R, Loebach J, Horan N, Min Ge, Thompson C, Yan L and Kahne D 1997 Polyvalent binding to carbohydrates immobilized on an insoluble resin; *Proc. Natl. Acad. Sci USA* **94** 10554–10559
- Lonngren J and Goldstein I 1978 Carbohydrate antigens: coupling melibionnic acid to bovine serum albumin using water-soluble carbodiimide; *Methods Enzymol.* **50** 160–162
- Majumdar M and Datta K 1998 Assignment of cDNA encoding hyaluronic acid binding protein 1 to human chromosome 17 p12-13; *Genomics* **51** 476–477
- Mego J L and Mcqueen J D 1995 Further studies on the degradation of injected [¹³¹I] albumin by secondary lysosomes of mouse liver; *Biochem. Biophys. Acta* **100** 166–173

- Parker A A, Kahmann J D, Howat S L T, Bayliss M T and Day A J 1998 TSG-6 interacts with hyaluronan and aggrecan in a pH-dependent manner via a common functional element: implications for its regulation in inflamed cartilage; *Fed. Eur. Biochem. Soc. Lett.* **428** 171–176
- Ranganathan S, Ganguly A K and Datta K 1994 Evidence for presence of hyaluronan binding protein on spermatozoa and its possible involvement in sperm function; *Mol. Reprod. Dev.* **38** 69–76
- Stahl P D 1990 The macrophage mannose receptor: current status; *An. J. Respir. Cell Mol. Biol.* **2** 37–52
- Towbin H, Staehelin T and Fordon J 1979 Electrophoretic transfer of proteins from polyacrylamide gels to nitrocellulose sheets: procedure and some applications; *Proc. Natl. Acad. Sci. USA* **76** 4350–4354
- Tulsiani D R P, Yoshida-Komiya H and Araki Y 1997 Mammalian fertilization: A carbohydrate-mediated event; *Biol. Reprod.* **57** 487–494
- White T K, Zhu Q and Tanzer M L 1995 Cell surface calreticulin is a putative mannoside lectin, which triggers mouse melanoma cell spreading; *J. Biol. Chem.* **270** 15926–15929
- Youssef H M, Doncel G F, Bassiouni B A and Acosta A A 1996 Mannose binding site on human spermatozoa and sperm morphology; *Fertil. Steril.* **66** 640–645

MS received 9 March 2001; accepted 2 May 2001

Corresponding editor: SEYED E HASNAIN